Rapid switch in monsoon-wind induced surface hydrographic conditions of the eastern Arabian Sea during the last deglaciation.

Title: Rapid switch in monsoon-wind induced surface hydrographic conditions of the eastern Arabian Sea during the last deglaciation.

Arun Deo Singh[1], Simon J.A. Jung[2], Pallavi Anand[3], Dick Kroon[4], Raja S. Ganeshram[5]

1 Arun Deo Singh (*Corresponding author*)
Department of Geology, Banaras Hindu University, Varanasi-221005, India
Email: arundeosingh@yahoo.com
Tel: +91-542-2366070, Fax: +91-542-2369425

2 Simon J. A. Jung
School of GeoSciences, Grant Institute, University of Edinburgh, The King,s Buildings,
West Mains Road, Edinburgh EH9 3JW, UK
Email: simon.jung@ed.ac.uk

3 Pallavi Anand
Department of Environment, Earth and Ecosystems, The Open University,
Milton Keynes, MK76AA, UK
Email: pallavi.anand@open.ac.uk

4 Dick Kroon
School of GeoSciences, Grant Institute, University of Edinburgh, The King,s Buildings,
West Mains Road, Edinburgh EH9 3JW, UK
Email: dkroon@staffmail.ed.ac.uk

5 Raja S. Ganeshram
School of GeoSciences, Grant Institute, University of Edinburgh, The King,s Buildings,
West Mains Road, Edinburgh EH9 3JW, UK
Email: r.ganeshram@ed.ac.uk

Rapid switch in monsoon-wind induced surface hydrographic conditions of the eastern Arabian Sea during the last deglaciation

ABSTRACT

Surface water hydrography in the Arabian Sea is primarily governed by the Asian monsoon wind system. Changes in the composition of fossil planktic foraminiferal assemblages and sea surface temperatures (SST) in sediment core SK17, retrieved from offshore of central India, are used to decipher past changes in sea-surface hydrographic conditions linked mainly to the winter monsoon winds. The planktic foraminiferal assemblage and the SST records indicate a rapid switch in sea-surface hydrographic conditions around 17.5 ka BP marking the end of last glacial period. The data show that intensified winter winds during 17.5 to 23.5 ka BP, resulted in nutrient injection into surface waters and eutrophic conditions, mainly through deep vertical mixing and/or moderate upwelling; and reduction in winter wind intensity caused stratification characterized by the high tropical SST since 17.5 ka BP. The timing of the rapid switch in seawater conditions caused by a drop in strength of winter monsoon winds is coeval with the cold climate excursion in the northern hemisphere (Heinrich Event 1), suggesting that the two areas are climatically linked.

Keywords: Arabian Sea; hydrography; winter monsoon; last deglaciation; Heinrich Event

1. Introduction

In the Arabian Sea, seasonally reversing air flow of the Asian monsoon produces spatial changes in surface circulation, hydrography and biological productivity. Through time, changes in the composition of planktic foraminiferal assemblages and sea surface temperatures largely reflect the history of upper water column conditions in response to changes in direction and/or strength of seasonal monsoon winds. Previous paleoceanographic studies using fossil planktic foraminifera were focused mainly on the western and northern regions predominantly influenced by the southwest (summer) monsoon. These studies have provided crucial insights into the

processes controlling summer monsoon variability on orbital and sub-orbital scales (eg. Clemens et al., 1991; Anderson and Prell, 1993; Venec-Peyre et al., 1995; Naidu and Malmgren, 1996; Reichart et al., 1998; von Rad et al., 1999; Venec-Peyre and Caulet, 2000; Jung et al., 2002; Gupta et al., 2003). However, high resolution planktic foraminiferal records from the eastern Arabian Sea, a region sensitive to the winter (northeast) monsoon circulation, are scarce. Therefore, our understanding of winter monsoon variability and associated changes in sea-surface hydrography particularly remains poor.

Previous studies have shown that wind driven changes in productivity and sea surface temperatures (SST) occurred at the millennial-scale in the western and northern Arabian Sea (e.g. Schulz et al., 1998; Ivanochko et al., 2005). Summer monsoon wind-induced upwelling generally reduced in the western and northern Arabian Sea during the glacial period, and particularly during extreme cold phases (Heinrich Events) in the northern hemisphere (Sirocko et al., 1993; Schulz et al., 1998; Ivanochko et al., 2005; Anand et al., 2008; Singh et al., 2011). The pattern of changes in surface hydrography of the eastern Arabian Sea, however, may well be different from those in the western and northern Arabian Sea, because of the dominant influence of winter monsoon winds in this area. At present, the winter winds cause shallow vertical mixing and sporadic upwelling along the central coast of India (Colborn, 1975; Zhang, 1985; Madhupratap et al., 1996; Schott and McCreary, 2001). Stratification of the surface waters occurs in summer because of increased fluvial runoff over the eastern Arabian Sea during the rainy summer season. In recent years, attempts have been made to study millennial-scale productivity variations in the eastern Arabian Sea influenced by seasonal monsoon air flow intensities, based on changes in the planktic foraminifera (Singh et al., 2006, 2011) and coccolithophore assemblages (Cabarcos et al., 2014). Changes in the upper water column structure through time, however , relating to millennial-scale variations in monsoon winds have not been studied in detail for the late glacial – Holocene.

We present planktic foraminiferal assemblage and Mg/Ca based SST records from sediment core SK 17 retrieved off Goa. This core provides a continuous record of upper ocean conditions in the eastern Arabian Sea during the last 30 ka BP. In particular, the reconstructions reveal millennial- scale changes in trophic conditions of the upper water column influenced by seasonal monsoon (summer vs winter) air flow intensities since the Last Glacial Maximum

(LGM). We explore links between these monsoon-induced air flow changes, global climate and deep-sea circulation.

2. Oceanographic Setting

Surface ocean circulation along the west coast of India is driven by seasonally reversing monsoon winds. Between June and September, SW monsoon winds prevail over the Arabian Sea (Fig. 1a). During this season, the West Indian Coastal Current (WICC) flows southward along the eastern margin of the Arabian Sea and joins the eastward flowing Southwest Monsoon Current (SMC) in the southeastern Arabian Sea (Schott and McCreary, 2001). Locally, high precipitation and runoff from the Western Ghats during the summer leads to a stratified surface water (Joseph and Freeland, 2005). The fluvial runoff supplies nutrient into surface waters, which can induce a local increase in productivity (Cabarcos et al., 2014). Further south, weak upwelling occurs along the southwest coast of India (south of 10^0 N) during this season (Sharma, 1966; Wyrtki, 1973; Naidu et al., 1999) resulting in the presence of moderately cold, nutrient-rich surface water in the region (Fig. 1a,b) .

During winter (December to March), the wind flow reverses and the NE monsoon prevails (Fig. 1a). Because of the reversed air flow, a cyclonic circulation develops causing weak and sporadic upwelling along the coasts off Pakistan and India (Colborn, 1975; Zhang, 1985; Bauer *et al.*, 1991). The cool and dry NE monsoon winds intensify evaporation, leading to surface cooling and vertical mixing in the eastern Arabian Sea, north of 10^0 N (Fig. 1b) [Banse and McClain, 1986; Madhupratap et al., 1996; Kumar et al., 2000]. The vertical mixing leads to a mild increase in primary productivity (Shalin, 2017). During this time, the WICC reverses and the Northeast Monsoon Current (NMC) transports waters from the Bay of Bengal (BOB) into the southeastern Arabian Sea up to 13^0 N (Sarma, 2003).

3. Material and Methods

Gravity core SK17 was retrieved from the sea bed off the central western Indian margin off Goa from 840 m water depth (Lat.15^0 15 ' N and Long. 72^0 58 ' E; core length 470 cm) during the ORV Sagar Kanya Cruise in 1999 (Fig.1). The sediment sequence is characterized by alternating

dark-coloured laminated and light-coloured bioturbated layers, free of gravity flows (Singh et al., 2006). Today the core site is well above the Calcite Compensation Depth (Belyaeva and Burmistrova, 1984). Singh et al. (2006) have evaluated dissolution effects on planktic foraminiferal tests in sediments of core SK 17. The results indicate that there is no evidence of significant dissolution of the tests over the last 30 ka BP.

The core was sampled every 1 cm interval up to one meter and further at 2 cm regular intervals. Alternate samples at 2 to 4 cm intervals were used in this study for planktic foraminiferal census counts. Dried sediments were washed over a 63 μm screen. The resulting dry residues were sieved over a 125 μm screen. Census counts of planktic foraminifera were made on the >125 μm fraction. The taxonomy of the planktic foraminifera is based on Kennett and Srinivasan (1983) and Hemleben et al. (1989). The relative abundance (%) of each species was calculated and plotted against depth to illustrate the down-core distribution patterns. In order to explain interrelationships in a multivariate database by the presence of a few key factors, we carried out Q mode factor analysis on the planktic foraminiferal relative abundances, using the SPSS 10.0. All species with a relative abundance > 2 % were included in this analysis (Table 1). Nitrogen isotopes ($\delta^{15}N$) were measured using a CE Instruments NA 2500 Elemental Analyser interfaced with a VG PRISMIII stable isotope spectrometer in continuous flow mode with helium career gas. The standard used is atmospheric nitrogen. The precision of measurement is $\pm$ 0.2 per mil. In addition to our new data (foraminiferal assemblage and $\delta^{15}N$ records), we also include previously published Mg/Ca -SST and $\delta^{18}Ow$ time series (Anand et al., 2008), the C_{org} record (Singh et al., 2006) and the aragonite record (Singh, 2007) of the same core SK 17. A section of the foraminiferal data (abundance ratio of *Globigerinoides ruber* and *Globigerina bulloides* and abundance total of fertile species viz. *G. bulloides, G. falconensis , G. glutinata* and *Neogloboquadrina dutertrei*) has been published earlier (Singh et al., 2011). The age model for core SK 17 is based on 26 AMS ^{14}C dates and has been published previously (Singh et al., 2011). The AMS^{14}C dates are based on monospecific samples of *Globigerinoides ruber*. Further details on the chronology are given in Singh et al. (2011).

4. Results

4.1. Planktic foraminiferal census counts

In total, 27 planktic foraminiferal species were found in core SK 17. The most abundant species, accounting on average for more than 80 % of the assemblage are: *Globigerinoides ruber* (26 %), *Globigerinita glutinata* (14.5 %), *Globigerina bulloides* (9.5 %), *Neogloboquadrina dutertrei* (9 %), *Globigerinoides quadrilobatus* (6 %), *Gobigerina falconensis* (5.5 %), *Globigerinoides sacculifer* (4 %), *Globorotalia menardii* (4 %), and *Pulleniatina obliquiloculata* (4 %). The relative abundance records of these species are shown in Fig. 2. The faunal record reveals that the planktic foraminiferal assemblages of the core are generally characterized by predominance of the *G. ruber* - *quadrilobatus* - *sacculifer* group (> 40 %). The cumulative abundance of these three species shows minima in the period 17.5 – 23.5 ka BP and the late Holocene (Fig. 2).

G. bulloides is an important species of the faunal assemblages of core SK17 with minimum concentrations of 4 % and maximum concentrations of up to 21 %. Its abundance maxima occur during the periods 22.5 - 23.5 ka BP and 18 -19 ka BP (Fig. 2). The abundance pattern of *G. falconensis* generally follows that of *G. bulloides* (Fig. 2). *G. glutinata* is another significant species, its relative abundance varies between 2 and 25 % (Fig. 2). This species shows high abundances during the periods 18 - 22 ka BP and 27 - 28 ka BP, and in the late Holocene (Fig. 2).

Other important taxa of the assemblages are *N. dutertrei, G. menardii* and *P. obliquiloculata*. The relative abundance of *N. dutertrei* varies between 4 % and 17 %. This species shows its maximum abundance during the period 17.5 – 23.5 ka BP. Its abundance decreases rapidly from 17.5 ka BP, followed by an increase at around 14 ka BP (Fig. 2). The relative abundance pattern of *G. menardii* broadly follows that of the *N. dutertrei* pattern, although it shows a more gradual decline in abundance from 17.5 ka BP onward, eventually disappearing around 15 ka BP. *P. obliquiloculata* shows a broad abundance maximum in the period 10.5 - 14 ka BP (Fig. 2).

4.2. Q mode factor analysis on planktic foraminifera

Multivariate analysis provides information on interspecies relationships and their dependency on varying environmental factors (e.g. Kroon, 1988; Caulet et al., 1992; Venec-

Peyre et al., 1995; Cayre et al., 1999; Venec-Peyre and Caulet, 2000). The factor analysis of planktic foraminiferal assemblages of core SK 17 results in three distinct groups of species, together accounting for 93 % of the total variance (Table 1). Factor 1 describes almost 40 % of the variance.

The highest-positive score of Factor 1 is attributed to *G. ruber*. Other important species having positive scores are *P. obliquiloculata* and *G. quadrilobatus*. These species are common in warm tropical surface waters and have adapted to nutrient-poor, oligotrophic water conditions (Bé and Tolderlund, 1971; Cullen, 1981; Cullen and Prell, 1984; Kroon, 1988). Factor 2 describes 35 % of the total variance. High positive scores of *G. bulloides, G. glutinata, G. falconensis* and *N. dutertrei* characterise Factor 2. These species prefer nutrient-rich, eutrophic water conditions, such as in a tropical upwelling environment (Bé and Tolderlund, 1971; Cullen, 1981; Cullen and Prell, 1984; Kroon, 1988). These species live mainly in the mixed layer except for *N. dutertrei* that lives in the thermocline during the adult phase (Sautter and Thunell, 1991; Ravelo and Fairbanks, 1992). Factor 3 describes 18 % of the total variance. This factor is dominated by positive scores of *G. glutinata*, with secondary contributions from *G. ruber*, *G. menardii* and *G. sacculifer*. Significantly, *G. bulloides, G. falconensis* and *N. dutertrei* (important contributors of Factor 2) have negative scores in Factor 3. We interpret the assemblage that contributes with positive scores to Factor 1 as the 'assemblage representing oligotrophic conditions in the mixed layer associated with surface water stratification' and the assemblage that contributes with positive scores to Factor 2 as the 'assemblage representing eutrophic conditions in the mixed layer associated with vertical mixing and/or upwelling '(eg. Venec-Peyre et al., 1995; Venec-Peyre and Caulet, 2000). The assemblage of Factor 3 appears to characterise small variations in mixed layer trophic conditions. These are of minor importance, because the assemblages of Factors 1 and 2 account for most of the total variance.

5. Discussion

5.1. Planktic foraminifera reflect mixed layer nutrient status and productivity

The multivariate statistical approach, employing abundance records of planktic foraminifera, provides a way of connecting groups of species to environmental parameters. In the

case of core SK17, the first two factors describe 75% in the data set, where two distinct planktic foraminiferal assemblages connect to two modes of ocean conditions related to the nutrient state of the mixed layer with implications for productivity. The species, dominant on the positive side of the first factor are *G. ruber, P. obliquiloculata, G. quadrilobatus* and *G. sacculifer*. These species are common in nutrient-poor, oligotrophic conditions, mainly in the mixed layer of highly stratified waters, such as in tropical gyre systems (Bé and Tolderlund, 1971; Ravelo and Fairbanks, 1992). The species *G. bulloides, G. glutinata, G. falconensis* and *N. dutertrei*, dominate on the positive side of Factor 2. These species are common in nutrient-rich, eutrophic conditions in highly mixed waters, such as tropical upwelling areas and regions of deep vertical mixing. Therefore, the two planktic foraminiferal assemblages dominant in the first two factors describe perfectly two contrasting water mass conditions regarding upper water column structure and nutrient concentration in the tropical Arabian Sea. Distribution patterns of these two assemblages in core SK 17 reveal monsoon driven periods of alternating oligotrophic and eutrophic surface waters in the region resulting from changes in the upper water column structure from a stratified to a mixed surface ocean. Today, seasonal productivity patterns in the eastern Arabian, particularly north of 10^0 latitude near the location of core SK 17 are governed by the seasonal winter monsoon winds that induce vertical mixing and sporadic upwelling and summer monsoon precipitations that induce surface water stratification (Madhupratap et al., 1996; Joseph and Freeland, 2005). Therefore, the alternating planktic foraminiferal assemblages, described by Factors 1 and 2, should reflect oceanic conditions associated with changes mainly in the intensity of the winter monsoon winds through time (Fig. 3) given the position of core SK 17 in the eastern Arabian Sea.

5.2. Changes in water column structure during key periods over the last 30 ka BP

<u>The last glacial period 17.5 - 23.5 ka BP</u>

High abundance of the eutrophic species assemblage (*G. bulloides, G. glutinata, G. falconensis, N. dutertrei*), described by the Factor 2, in the period 17.5 - 23.5 ka BP (Fig. 3), suggests not only nutrient-rich conditions in the surface mixed layer but also in the thermocline, where adult populations of *N. dutertrei* reside. Presence of this assemblage strongly indicates

periods of high productivity associated with nutrient supply to surface waters either due to deep vertical mixing or upwelling or a combination of both, which is further corroborated by the remarkably low SST based on Mg/Ca ratios in shells of *G. bulloides* (Anand et al., 2008) and high C_{org} content (Singh et al., 2006)[Fig. 3]. Heavier $\delta^{15}N$ values during this interval also suggest high productivity conditions coupled with sluggish eastern boundary circulation and denitrification (Fig. 4) (Naqvi et al., 1998; Ivanochko et al., 2005). The combined set of data supports the notion that strengthened winter monsoon winds caused intense vertical mixing (eg. Emeis et al., 1995) leading to nutrient –rich subsurface water into the photic zone, which in turn fueled high productivity between 17.5 and 23.5 ka BP. Moreover, upwelling may have also been enhanced during this interval. Today, the convective vertical mixing is the dominant driver of eutrophic conditions in winter monsoon season, and it was probably the main driver in the glacial period; but possibility of somewhat enhanced upwelling cannot be ruled out. At this stage, however, it is difficult to separate the two physical processes resulting in eutrophic conditions. This finding is in line with earlier publications (eg. Rostek et al., 1997; Ivanova et al., 2003; Singh et al., 2011; Cabarcos et al., 2014).). It is intriguing to note that within the period 17.5 - 23.5 ka BP, G. *bulloides* concentrations declined for a short spell around 20 - 21 ka BP (Fig. 2). This decline of *G. bulloides* abundance probably does not indicate a complete loss of productivity, because concomitant increases in abundances of other nutrient loving species like *G. glutinata* and *N. dutertrei* occurred. This finding probably suggests that nutrient availability in surface waters remained relatively high during this period but perhaps subsurface waters, brought to the surface, were not sufficiently enriched in nutrients for *G. bulloides* populations to thrive, whilst the other eutrophic species flourished. The process of nutrient injection was probably related to shallow winter convective mixing rather than upwelling, which generally brings nutrient from deeper thermocline levels. Interestingly, such subtle changes in the eutrophic species assemblage seem to support the notion that each species within the assemblage has a unique response to changes in environmental conditions. Further studies in the modern ocean will be able to shed more lights in our understanding of planktic foraminiferal responses, leading to improved interpretation of species abundance records in paleoceanographic reconstructions.

<u>Rapid change in hydrographic conditions during the last deglaciation 15 – 17.5 ka BP</u>

The planktic foraminiferal record of core SK 17 shows major changes during the last deglaciation commencing around 17.5 ka BP. The abundances of species, indicative of eutrophic waters (Factor 2), declined rapidly accompanied by concomitant increase in mixed layer oligotrophic species (Factor 1), implying a change to oligotrophic waters prevailing during the deglaciation (17.5 - 15 ka BP). This finding suggests a shift from a dominant nutrient-rich productive environment to one characterized by relatively nutrient-poor stratified surface waters . The new data are in line with a significant increase in surface temperatures of the mixed layer (Anand et al., 2008) and lower C_{org} concentration (Singh et al., 2006), jointly supporting the notion of low productivity during the deglaciation between 17.5 and 15 ka BP (Figs. 3,4). The lighter values of $\delta^{15}N$ during this interval also imply low productivity related to nutrient depletion in subsurface water, as compared to that of during the LGM (Fig 4). Thus, the changes in planktic foraminiferal assemblage composition, SST, C_{org} content and $\delta^{15}N$ suggest a rapid change in surface oceanic conditions, probably triggered by a change in strength of winter monsoon winds around 17.5 ka BP: strong winter monsoon winds were replaced by moderate or weak winter monsoon winds, reducing nutrient availability in surface waters.

The timing of this switch in intensity of winter monsoon winds is synchronous with Heinrich Event 1 (H1), a cold event in the northern hemisphere, when the large-scale deposition of ice rafted sediments occurred (Bond and Lotti, 1995). We are confident that the timing of the winter monsoon weakening around 17.5 ka BP is well constrained by AMS ^{14}C-dates in core SK 17 and matches the timing of H1 within the uncertainties associated with radiocarbon dating. Reichart et al. (1998) inferred intensified winter northeasterly wind induced convective mixing in the northern Arabian Sea during this time. In such scenario, productivity would be maintained during H1, but, in contrast, the planktic foraminiferal record from core SK 17 suggests reduced productivity. Others suggest that variations in nutrient supply through intermediate waters may have played a role in this reduction of productivity (e.g. Ziegler et al., 2010). However, this would still require a mechanism that transfers intermediate waters across the thermocline to the surface. The SST data from core SK 17 show evidence of a change from cold to warm surface waters during the time period of H1, confirming a change from deep vertical mixing and/or upwelling to stratified waters. Thus, although nutrient content of deeper waters may have played

some role in productivity changes (Ziegler et al., 2010), strength of winter monsoon winds likely dropped during H1.

Similarly, reduced strength of winter monsoon winds resulting in stratified surface waters and low productivity conditions during H1, can also be observed in the period 23.5 – 24.5 ka BP (equivalent to the North Atlantic H2), at least in this part of the Arabian Sea. The reduction in productivity, however, was less prominent than during H1. The coupled cooling in the northern hemisphere, reduction of productivity and warming of surface waters in the eastern Arabian Sea occurred repeatedly during Heinrich Events in the glacial period (see also Singh et al., 2011).

In contrast to our conclusion of a more stratified upper water column, low productivity and weaker winter monsoon winds in the period 15-17.5 ka BP based on foraminifer assemblages, SST and $\delta^{15}N$ records (Fig. 4), Cabarcos et al. (2014) suggested increased productivity and stronger winter monsoon winds in this period based on coccolith assemblage data in the same core (Fig.4). Indeed, the coccolith assemblage data (Factor 1, the productivity proxy as defined by Cabarcos et al., 2014) indicate relatively high productivity in the prolonged period 17.5-10 ka BP. Thus, the coccolithophore driven productivity remained largely unaffected during the cold H1 event. A wider discussion on the coupling of low productivity events in the Arabian Sea and cold events (Heinrich Events) in the northern hemisphere may be useful to speculate why the coccolith and the foraminifer assemblage results are different. The changes in the planktic foraminifer assemblage, SST and $\delta^{15}N$ records are in concert with northern hemisphere climate events, not only during H1, but also during H2, and in the period LGM to H1 (Fig. 4). The low productivity Arabian Sea events are clearly linked with the Heinrich cold periods in the northern hemisphere. This is not necessarily new, because this pattern of coupling between Arabian Sea low productivity and northern hemisphere cold climate events has been previously reported using a wide variety of proxy data series in cores from across the Arabian Sea (Schulz et al., 1998; Altabet et al., 2002; Ivanochko et al., 2005; Singh et al., 2006, 2011). It is intriguing to note that a record of changes in dinoflagellate assemblage data, from another deep core offshore Goa (water depth; 1807 m), suggested also low productivity during H1 (Narale et al., 2015). The weak response of coccolithophores to millennial-scale climate change as evident in figure 4 is anomalous. The coccolithophores dwelling in the mixed layer may have a specific response to nutrient supply (Tarran et al., 1999; Le Mézo et al., 2017). Perhaps coccolithophore abundances

and assemblage composition are sensitive to nutrient supply from the continent either by runoff/river or wind (Patil and Singh, 2013, Cabarcos et al., 2014), much more so than other primary producers. Furthermore, coccolithophores are also known to be sensitive to salinity and turbidity of surface waters (McIntyre and Bè, 1967; Baumann et al., 2005). The location of core SK 17 is close to the coast where large variability in salinity and turbidity occurs. Intriguingly, the reconstructed δ^{18}Ow values (salinity related) show large swings in the glacial-deglaciation period (Fig 4), which may have played a role in the abundance changes of the coccolithophores. Although nutrients, salinity and turbidity may explain the anomalous behavior of coccolithiphores ecology, the precise reason for this remains unclear.

The Holocene surface hydrography

Low abundances of planktic foraminifera that contribute positively to Factor 2, and corresponding high abundances of species that contribute positively to Factor 1 in conjunction with low C_{org} content and high Mg/Ca-based SST collectively suggest that a strongly stratified upper water column prevailed during most of the Holocene except for the last 2.5 ka BP (Fig. 3). A moderate increase in productivity over the last 2.5 ka BP probably marks the establishment of modern conditions of weak winter vertical mixing and /or sporadic upwelling, driven by slightly enhanced northeasterly winter monsoon winds in the eastern Arabian Sea. The coccolithophore record of Cabarcos et al. (2014) indicates stratified surface water and relatively low productivity during the Holocene.

5.3. Abundance variations of G. menardii : implications for changes in thermocline ventilation

Deep dwelling planktic foraminifera may reveal thermocline conditions in the eastern Arabian Sea over the last 30 ka BP. Populations of *G. menardii*, *N. dutertrei*, and *P. obliquiloculata* tend to flourish in areas where a deep chlorophyll maximum occurs (Sexton et al, 2011), although each of these species has adapted to slightly different ecological niches which are yet to be fully deciphered. Despite this principle limitation, there is agreement that *G. menardii* thrives in thermocline waters associated with the so-called deep chlorophyll maximum

where oxygen levels are relatively low and nutrient levels are high (Karstensen et al., 2008; Sexton et al, 2011).

In core SK 17, the abundance pattern of *G. menardii* is broadly similar to that of *N. dutertrei*, a thermocline, eutrophic species flourishing in upwelling conditions (Fig. 2). During the periods of monsoon winds induced high surface productivity, upper thermocline waters are enriched in nutrients and depleted in oxygen , a condition favourable for *G. menardii*. A change in ventilation conditions of intermediate waters may lead to variation in oxygen levels at lower thermocline depth, thus affecting *G. menardii* abundance. Hence, *G. menardii* populations in the eastern Arabian Sea, though primarily governed by the productivity, may have been significantly influenced by intermediate water ventilation influencing lower thermocline conditions in the eastern Arabian Sea (Naidu et al., 2014).

High concentrations of *G. menardii* between 17. 5 and 23.5 ka BP suggest poorly ventilated thermocline waters, enriched in nutrients (Fig. 2 and Fig. 5). Notably, the abundance of *G. menardii* declined conspicuously during 15- 17.5 ka BP, but more intriguingly, the *G. menardii* population almost disappeared just after the H1. It appears that these changes are related to the ventilation history of intermediate waters combined with the productivity variations. Interestingly, during other North Atlantic cold phases (Younger Dryas and Heinrich 2 Events) *G. menardii* disappeared (Fig. 5). Other evidence for ventilation of the thermocline can be found in geochemical data. For instance, aragonite concentrations can be very indicative of changes in the ventilation state of the intermediate waters (Singh, 2007; Naidu et al., 2014). Old water becomes more corrosive and dissolves aragonite, due to increased CO_2 content that lowers the pH of the waters. The intervals of *G. menardii* abundance minima correspond very well with the maxima in aragonite content in the core SK17 (Fig. 5). This finding suggests that *G. menardii* disappeared during phases of enhanced ventilation pointing to periods of repeated collapses of the oxygen minimum zone. Most likely increased ventilation of the deep waters in the Arabian Sea during Heinrich events was triggered by world-wide global climate changes. Jung et al. (2010) showed profound evidence of changes in ventilation state of the intermediate waters in the western Arabian Sea. They concluded that intensified inflow of Antarctic Intermediate Water to Arabian Sea probably ventilated the thermocline waters during northern hemisphere cold phases. Thus, this likely happened in the eastern Arabian Sea in a similar way, which caused the demise of the *G. menardii* populations. Interestingly, reduction in *G. menardii*

populations occurred during the Heinrich events, but complete collapse of these populations occurred slightly later when the northern hemisphere was still cold, and the populations recovered again during the warming phase.

6. Conclusions

Variations in the composition of planktic foraminiferal assemblages in core SK 17 from the eastern Arabian Sea are used to reconstruct changes in upper water column structure over the last 30 ka BP. Down-core variations in faunal records (species abundances, factor loadings) correlate with fluctuations of C_{org} % and SST. While strong monsoon winter winds drove deep vertical mixing and/or moderate upwelling, in the period 17.5 - 23.5 ka BP, high abundance of *G. menardii* during this period suggests that thermocline waters were poorly ventilated.

At 17.5 ka BP, a rapid decline in productivity and nutrient availability occurred with a concomitant increase in SST, implying a change towards stratification of surface waters and reduced winter monsoon winds. The *G. menardii* abundance record supports the notion that the upper thermocline waters became ventilated during this period, but ventilation improved further between 15 and 17.5 ka BP. These changes are synchronous with northern hemisphere climate changes. Notably, the reduction in winter monsoon intensity, increased SST's, and better ventilation occurred simultaneously with the onset of Heinrich event (H1), showing climate connections between the two areas, through wind systems but also through flow regimes of intermediate waters.

The faunal data further suggest a moderate increase in winter wind induced vertical mixing and/or sporadic upwelling to modern levels since 2.5 ka BP.

Acknowledgements

This research was supported by funding to A.D.S. and by the GBP-ISRO (India) and from the DST (New Delhi). Support to P.A. from NERC is also acknowledged. We thank the anonymous reviewers for the constructive comments.

References

Altabet, M.A., Higginson, M.J., Murray, D.W., 2002. The effect of millenial-scale changes in high frequency Arabian Sea denitrification on atmospheric CO_2. Nature 415, 159–162.

Anand, P., Kroon, D., Singh, A.D., Ganeshram, R.S., Ganssen, G., Elderfield, H., 2008. Coupled sea surface temperature-seawater $\delta^{18}O$ reconstructions in the Arabian Sea at the millennial scale for the last 35 ka. Paleoceanography 23, PA4207, doi:10.1029/2007PA001564.

Anderson, D.M., Prell, W.L., 1993. A 300 kyr record of upwelling off Oman during the late Quaternary; evidence of the Asian southwest monsoon. Paleoceanography 8, 193-208.

Banse, K., McClain, C.R., 1986. Winter blooms of phytoplankton in the Arabian Sea as observed by the Coastal Zone Color Scanner. Marine Ecology Progress Series 34, 201-211.

Bauer, S., Hitchcock, G.L., Olson, D.B., 1991. Influence of monsoonally-forced Ekman dynamics upon surface-layer depth and plankton biomass distribution in the Arabian Sea. Deep-Sea Research Part A 38 (5), 531–553.

Baumann, K.-H., Andruleit, H., BöckeL, B., Geisen, M., Kinkel, H., 2005. The significance of extant coccolithophores as indicators of ocean water masses, surface water temperature, and paleoproductivity: a review. Paläontologische Zeitschrift 79(1), 93–112.

Bè, A.W.H., Tolderlund, D.S., 1971. Distribution and ecology of living planktonic foraminifera in surface waters of the Atlantic and Indian Oceans. In: Funnel, B.M., Riedel, W.R. (eds.), The Micropaleontology of Oceans. Cambridge University Press, pp. 105-149.

Belyaeva, N.V., Burmistrova, I.I., 1984. Foraminiferal Lysocline and critical levels of carbonate sedimentation in the Indian Ocean. Litologiya i Poleznye Iskopaemye, Russian 6, 57-66.

Blunier, T., Brook, E.J., 2001. Timing of millennial-scale climate change in Antarctica and Greenland during the last glacial period. Science 291, 109-112.

Blunier, T., Chappellaz, J., Schwander, J., Dallenbach, A., Stauffer, B., Stocker, T.F., Raynaud, D., Jouzel, J., Clausen, H.B., Hammer, C.U., Johnsen, S.J., 1998. Asynchrony of Antarctic and Greenland climate change during the last glacial period. Nature 394, 739-743.

Bond, G.C., Lotti, R., 1995. Iceberg discharges into the north-Atlantic on millennial time scales during the last glaciation. Science 267(5200), 1005-1010.

Cabarcos, E., Flores, J.A., Singh, A.D., Sierro, F.J., 2014. Monsoonal dynamics and evolution of the primary productivity in the eastern Arabian Sea over the past 30 ka. Palaeogeography, Palaeoclimatology, Palaeoecology 411, 249–256.

Caulet, J.P., Venec-Peyre, M., Vergnaud-Grazzini, C., Nigrini, C., 1992. Variation of South Somalian upwelling during the last 160 ka: radiolarian and foraminifera records in core MD85674. In: Summerhays, C.P., Prell W.L., Emeis, K.C. (eds.), Upwelling Systems: Evolution since the Early Miocene. Geological Society Special Publication, London 64, pp. 379-389.

Cayre, O., Beaufort, L., Vincent, E., 1999. Paleoproductivity in the equatorial Indian Ocean for the last 260,000 yr: transfer function based on planktonic foraminifera. Quaternary Science Reviews 18, 337-342.

Clemens, S., Prell, W.L., Murray, D., Shimmield, G., Weedon, G., 1991. Forcing mechanisms of the Indian Ocean monsoon. Nature 353, 720-725.

Colborn, J.G., 1975. The thermal structure of the Indian Ocean. In: International Indian Ocean Expedition Monograph, University of Hawaii Press, Honolulu 2, pp. 173.

Cullen, J.L., 1981. Microfossil evidence for changing salinity in the Bay of Bengal over the last 20,000 years. Palaeogeography, Palaeoclimatology, Palaeoecology 35, 315-356.

Cullen, J.L., Prell, W.L., 1984. Planktonic foraminifera of the northern Indian Ocean: distribution and preservation in surface sediments. Marine Micropaleontology 9, 1-52.

Emeis, K.C., Anderson, D.M., Doose, H., Kroon, D., Schulz-Bull, D., 1995. Sea-surface temperatures and the history of monsoon upwelling in the Northwest Arabian Sea during the last 500,000 years. Quaternary Research 43(3), 355-361.

Gupta, A.K., Anderson, D.M., Overpeck, J.T., 2003. Abrupt changes in the Asian southwest monsoon during the Holocene and their links to the North Atlantic Ocean. Nature 421, 354-357.

Hemleben, C., Spindler, M., Anderson, O.R., 1989. Modern planktonic foraminifera. Springer-Verlag, New York, pp. 363.

Hemming, S.R., 2004. Heinrich events: Massive late Pleistocene detritus layers of the North Atlantic and their global climate imprint. Reviews of Geophysics 42, RG1005, doi:1029/2003RG000128.

Ivanochko, T.S., Ganeshram, R.S., Brummer, G-J.A., Ganssen, G., Jung, S.J.A., Moreton, S.G., Kroon, D., 2005. Variations in tropical convection as an amplifier of global climate change at the millennial scale. Earth and Planetary Science Letters 235, 302-314.

Ivanova, E., Schiebel, R., Singh, A.D., Schmiedl, G., Niebler, H.S., Hemleben, C., 2003. Primary production in the Arabian Sea during the last 135000 years. Palaeogeography, Palaeoclimatology, Palaeoecology 197, 61–82.

Joseph, S., Freeland, H.J., 2005. Salinity variability in the Arabian Sea. Geophysical Research Letters 32, L09607. doi:10.1029/2005GL022972

Jung, S.J.A., Davies, G.R., Ganssen, G., Kroon, D., 2002. Centennial-millennial scale monsoon variations off Somalia over the last 35 ka. In: Clift, P., Kroon, D. (eds.), Tectonic and Climatic Evolution of the Arabian Sea Region. Geological Society of London, Special Publication 195, pp. 341-352.

Jung, S.J.A., Kroon, D., Ganssen, G., Peeters, F., Ganeshram, R., 2010. Southern Hemisphere intermediate water formation and the bi-polar seesaw. PAGES news, 18 (1), 36-38.

Karstensen, J., Stramma, L., Visbeck, M., 2008. Oxygen minimum zones in the eastern tropical Atlantic and Pacific Oceans. Progress in Oceanography 77, 331-350.

Kennett, J.P., Srinivasan, M.S., 1983. Neogene planktonic foraminifera, a Phylogenetic Atlas. Hutchinson and Ross Publications, Pennsylvania, pp. 265.

Kroon, D., 1988. The planktic $\delta^{13}C$ record, upwelling and climate. In: Brummer, G-J.A., Kroon, D. (eds.), Planktonic Foraminifers as Tracers of Ocean-Climate History. Free University Press, Amsterdam, pp. 335-346.

Kumar, S.P., Madhupratap, M., Kumar, M.D., Gauns, M., Muraleedharan, P.M., Sarma, V.V.S. S., De Souza, S.N., 2000. Physical control of primary productivity on a seasonal scale in central and eastern Arabian Sea. Proceedings Indian Academy of Sciences (Earth and Planetary Science) 109, pp. 433-441.

Le Mézo, P., Beaufort, L., Bopp, L., Braconnot, P., Kageyama, M., 2017. From monsoon to marine productivity in the Arabian Sea: insights from glacial and interglacial climates. Climate of the Past 13, 759-778.

Madhupratap, M., Kumar, S.P., Bhattathiri, P.M.A., Kumar, M.D., Raghukumar, S., Nair, K.K. C., Ramaiah, N., 1996. Mechanism of the biological response to winter cooling in the northeastern Arabian Sea. Nature 384, 549-552.

Meese, D.A., Gow, A.J., Alley, R.B., Zielinski, G.A., Grootes, P.M., Ram, M., Taylor, K.C., Mayewski, P.A., Bolzan, J.F., 1997. The Greenland Ice Sheet Project 2 depth-age scale: Methods and Results. Journal of Geophysical Research 102 (26), 411-423.

McIntyre, A., Bè, A.H.W., 1967. Modern coccolithophores of the Atlantic Ocean-I. Placolith and cyrtoliths, Deep Sea Research 14, 561–597.

Naidu, P.D., Malmgren, B.A., 1996. A high-resolution record of late Quaternary upwelling along the Oman margin, Arabian Sea based on planktonic foraminifera. Paleoceanography 11, 129-140.

Naidu, P.D., Ramesh Kumar, M.R., Ramesh Babu, V., 1999. Time and space variations of monsoonal upwelling along the west and east coasts of India. Continental Shelf Research 19, 559-572.

Naidu, P.D., Singh, A.D., Ganeshram, R., Bharti, S.K., 2014. Abrupt climate-induced chages in carbonate burial in the Arabian Sea: Causes and consequences. Geochemistry, Geophysics, Geosystems 15, 1398-1406.

Naqvi, S.W.A., Yoshinari, T., Jayakumar, D.A., Altabet, M.A., Narvekar, RV., Devol, A.H., Brandes, J.A., Codispoti, L.A., 1998. Budgetary and biogeochemical implications of N_2O isotope signatures in the Arabian Sea. Nature 394, 462-464.

Narale, D.D., Naidu, P.D., Anil, A.C., Godad, S.P., 2015. Evolution of productivity and monsoonal dynamics in the eastern Arabian Sea during the past 68 ka using dinoflagellate cyst records. Palaeogeography, Palaeoclimatology, Palaeoecology 435, 193–202. http://dx.doi.org/ 10.1016/ j.palaeo.2015.06.006

Patil, S.K., Singh, A.D., 2013. New record of magnetic properties of Late Quaternary sediments from the Eastern Arabian Sea (off Goa): inferences on Palaeoclimate. In: Sinha, R., Ravindra, R. (eds.), Earth System Processes and Disaster Management. Springer, Berlin, pp. 113–121.

Ravelo, A.C., Fairbanks, R.G., 1992. Oxygen isotopic composition of multiple species of planktic foraminifera: Recorders of the modern photic zone temperature gradient. Paleoceanography 7, 815-831.

Reichart, G.J., Lourens, L.J., Zachariasse, W.J., 1998. Temporal variability in the northern Arabian Sea Oxygen Minimum Zone (OMZ) during the last 225,000 years. Paleoceanography 13, 607-621.

Rostek, F., Bard, E., Beaufort, L., Sonzogni, C., Ganssen, G., 1997. Sea surface temperature and productivity records for the past 240 kyr in the Arabian Sea. Deep-Sea Research Part II 44 (6–7), 1461–1480.

523 Sarma, V.V.S.S., 2003. Monthly variability in surface pCO_2 and net air-sea CO_2 in the Arabian
524 Sea. Journal of Geophysical Research 108: doi: 10.1029/2001JC001062.
525 Sautter, L.R., Thunell, R.C., 1991. Planktonic foraminiferal response to upwelling and seasonal
526 hydrographic conditions: sediment trap results from San Pedro Basin, Southern California
527 Bight. Journal of Foraminiferal Research 21, 347-363.
528 Schott, F.A., McCreary, J.P., 2001. The monsoon circulation of the Indian Ocean. Progress in
529 Oceanography 51 (1), 1-123.
530 Schulz, H., von Rad, U., Erlenkeuser, H., 1998. Correlation between Arabian Sea and Greenland
531 climate oscillation of the past 110,000 years. Nature 393, 54-57.
532 Sexton, P.F., Norris, R.D., 2011. High latitude regulation of low latitude thermocline ventilation
533 and planktic foraminifer populations across glacial-interglacial cycles. Earth and Planetary
534 Science Letters 311 (1-2), 69-81.
535 Shalin, S., Samuelsen, A., Korosov, A., Menon, N., Backeberg, B.C., Pettersson, L.H., 2017.
536 Delineation of marine ecosystem zones in the northern Arabian Sea using an objective
537 method. Biogeosciences Discussions, doi.org/10.5194/bg-2017-285.
538 Sharma, G.S., 1966. Thermocline as an indicator of upwelling. Journal of Marine Biological
539 Association of India 8, 8-19.
540 Singh, A.D., 2007. Episodic preservation of pteropods in the eastern Arabian Sea: monsoonal
541 change, oxygen minimum zone intensity and aragonite compensation depth. Indian Journal
542 of Marine Sciences 36(4), 378-383.
543 Singh, A.D., Kroon, D., Ganeshram, R.S., 2006. Millennial scale variations and OMZ intensity
544 in the eastern Arabian Sea. Journal of the Geological Society of India 68, 369-377.
545 Singh, A.D., Jung, S.J.A., Darling, K., Ganeshram, R., Ivanochko, T., Kroon, D., 2011.
546 Productivity collapses in the Arabian Sea during glacial cold phases. Paleoceanography 26,
547 PA3210, doi:1029/2009PA001923.
548 Sirocko, F., Sarnthein, M., Erlenkeuser, H., Lange, H., Arnold, M., Duplessy, J.-C., 1993.
549 Century-scale events in monsoonal climate over the past 24,000 years. Nature 364, 322-
550 324.
551 Tarran, G.A., Burkill, P.H., Edwards, E.S., Woodward, E.M.S., 1999. Phytoplankton community
552 structure in the Arabian Sea during and after the SW monsoon, 1994. Deep-Sea Research II
553 46, 655– 676.

Venec-Peyre, M.-T., Caulet, J.P., 2000. Paleoproductivity changes in the upwelling system of Socotra (Somali Basin, NW Indian Ocean) during the last 72,000 years: evidence from biological signatures. Marine Micropaleontology 40, 321-344.

Venec-Peyre, M.-T., Caulet, J.P., Vergnaud Grazzini, C., 1995. Paleohydrographic changes in the Somali Basin (5^0N upwelling and equatorial areas) during the last 160 kyr, based on correspondence analysis of foraminiferal and radiolarian assemblages. Paleoceanography 10, 473-491.

von Rad, U., Schulz, H., Riech, V., den Dulk, M., Berner, U., Sirocko, F., 1999. Multiple monsoon-controlled breakdown of oxygen-minimum conditions during the past 30,000 years documented in laminated sediments off Pakistan. Palaeogeography, Palaeoclimatology, Palaeoecology 152, 129-161.

Wyrtki, K., 1973. Physical oceanography of the Indian Ocean. In: Zeitzschel, B., Gerlach, S.A. (eds.), The Biology of the Indian Ocean. Springer-Verlag, New York, pp. 18-36.

Zhang, J., 1985. Living planktonic foraminifera from the eastern Arabian Sea. Deep Sea Research 32, 789-798.

Ziegler, M., Lourens, L.J., Tuenter, E., Hilgen, F., Reichart, G.-J., Weber, N., 2010. Precession phasing offset between Indian summer monsoon and Arabian Sea productivity linked to changes in Atlantic overturning circulation. Paleoceanography 25, PA3213, doi:10.1029/2009PA001884.

585 **Caption of Figures and Table**

586

587 Figure 1. Map showing the location of core SK17 off Goa. Schematic patterns of atmospheric
588 and oceanographic circulation; chlorophyll concentration (a); and sea surface temperature (b)
589 during the summer and winter monsoons (source Chl a: NASA/SeaWiFS; SST: NOAA).
590 Dominant wind direction (broken white lines) and main surface ocean circulation (white lines),
591 along the west coast of India during both seasons. WICC: West Indian Coastal Current; EICC:
592 East Indian Coastal Current; NMC: Northeast Monsoon Current; SMC: Southwest Monsoon
593 Current (Schott and McCreary, 2001).

594

595 Figure 2. Planktic foraminiferal (*G. ruber*) oxygen isotope record (Singh et al., 2006) and
596 relative abundances of important planktic foraminifera (*G. sacculifer, G. ruber,*
597 *G. quadrilobatus, G. bulloides, G. glutinata, G. falconensis, G. menardii, N. dutertrei* and
598 *P. obliquiloculata*). The grey bars on plot show timing and duration of the Younger Dryas (YD),
599 Heinrich 1 (H1), Heinrich 2 (H2) events (Hemming, 2004) and the Last Glacial Maximum
600 (LGM).

601

602 Figure 3. Records of variations in upwelling, productivity and surface water hydrographic
603 conditions. The Greenland ice core (GISP) record (Blunier and Brook, 2001; Blunier et al., *1998;*
604 Meese et al., 1997), Planktic foraminiferal (*G. ruber*) oxygen isotope record (Singh et al., 2006),
605 Mg/Ca sea surface temperature (G. bulloides) record [Anand et al., 2008], Records of Factor
606 loadings for planktic foraminifera (Factor 1 assemblage: non-upwelling and oligotrophic mixed
607 layer condition; Factor 2 assemblage: upwelling and eutrophic mixed layer condition), Organic
608 carbon (wt %) record. The grey bars on plot show timing and duration of the Younger Dryas
609 (YD), Heinrich 1 (H1), Heinrich 2 (H2) events (Hemming, 2004) and the Last Glacial Maximum
610 (LGM).

611

612 Figure 4. Comparison of proxy records for paleoproductivity (foraminifera Factor 2 and $\delta^{15}N$,
613 this study; coccolithophore Factor 1, Cabarcos et al., 2014); surface water stratification
614 (foraminifera Factor 1, this study; coccolithophore Factor 2, Cabarcos et al., 2014); and Mg/Ca-
615 temperature and seawater $\delta^{18}O$ records (Anand et al., 2008). The grey bars on plot show timing

and duration of the Younger Dryas (YD), Heinrich 1 (H1), Heinrich 2 (H2) events (Hemming, 2004) and the Last Glacial Maximum (LGM).

Figure 5. Record of changes in thermocline ventilation. Relative abundance of *Globorotalia menardii*, a deep dwelling thermocline species (abundance minima indicate enhanced thermocline ventilation and maxima indicate poor ventilation), Aragonite content (wt %) [Singh, 2007] in bulk sediment (aragonite maxima are related to enhanced ventilation of intermediate waters). The grey bars on plot show timing and duration of the Younger Dryas (YD), Heinrich 1 (H1), Heinrich 2 (H2) events (Hemming, 2004) and the Last Glacial Maximum (LGM).

Table 1: Matrix of Factor Scores of the three planktic foraminiferal Q mode Varimax Factors.

647 Table 1. Matrix of Factor Scores of the three planktic foraminiferal Q mode Varimax Factors

648

Species	Factor 1	Factor 2	Factor 3
G. bulloides	-0.09281	2.62695	-1.73499
G. falconensis	-0.1235	1.25701	-1.24476
G. rubescens	-0.39177	-0.3174	-0.0319
G. ruber	3.57825	0.45746	1.68678
G. triloba	0.3398	-0.83257	-0.54092
G.quadrilobatus	0.77084	-0.07831	-0.5717
G. sacculifer	-0.00678	-0.75962	0.85746
G. tenellus	-0.44166	-0.40246	0.17784
G. conglobatus	-0.34968	-0.64771	-0.117
O. universa	-0.19619	-0.43783	-0.35828
P.obliquiloculata	1.04239	-0.77031	-0.84219
G. glutinata	-1.35949	2.01315	2.75751
N. dutertrei	0.37635	1.22229	-0.66483
N. pachyderma	-0.4705	-0.60373	-0.14899
G. menardii	-0.8125	-0.05412	1.02115
G. ungulata	-0.57459	-0.63428	0.06838
G. hexagona	-0.50439	-0.64187	0.09511
G. aequiletaralis	0.10842	-0.14268	-0.38802
G. calida	-0.4244	-0.50237	-0.21181
G. venezuelana	-0.46781	-0.75161	0.19114

649

	% of Variance	Cumulative%
Factor 1	39.918	39.918
Factor 2	34.981	74.898
Factor 3	18.504	93.402

650

651

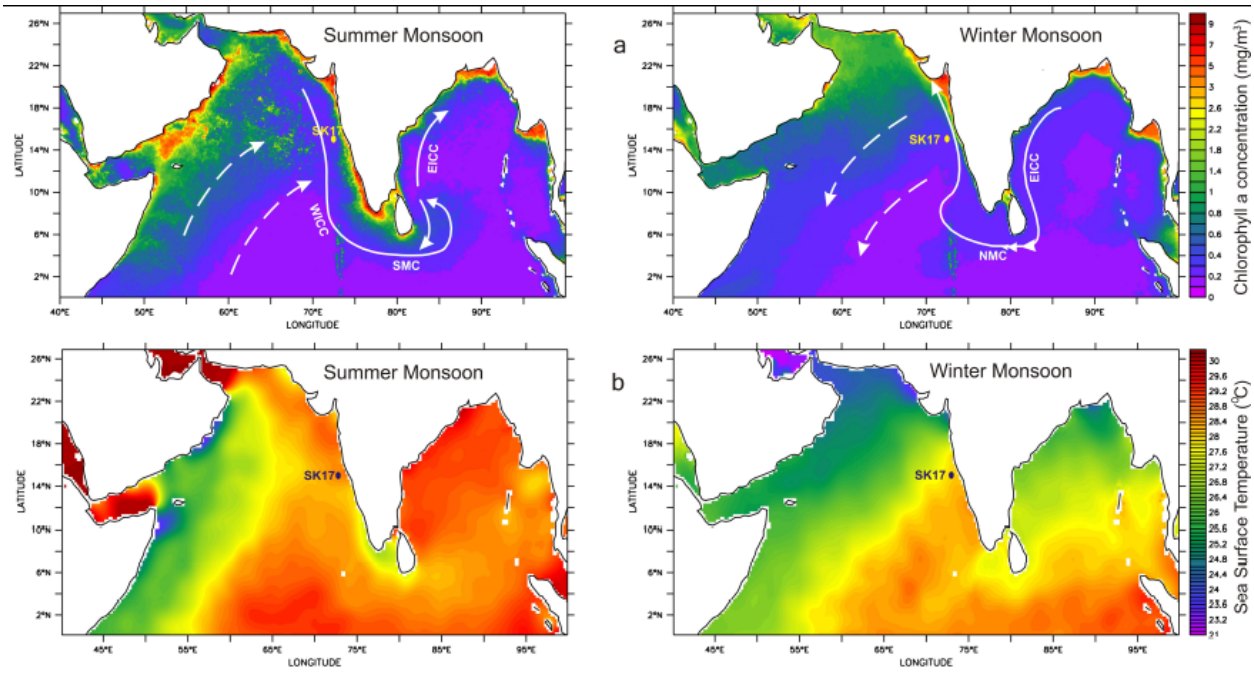

Figure 1 Singh et al

652

653

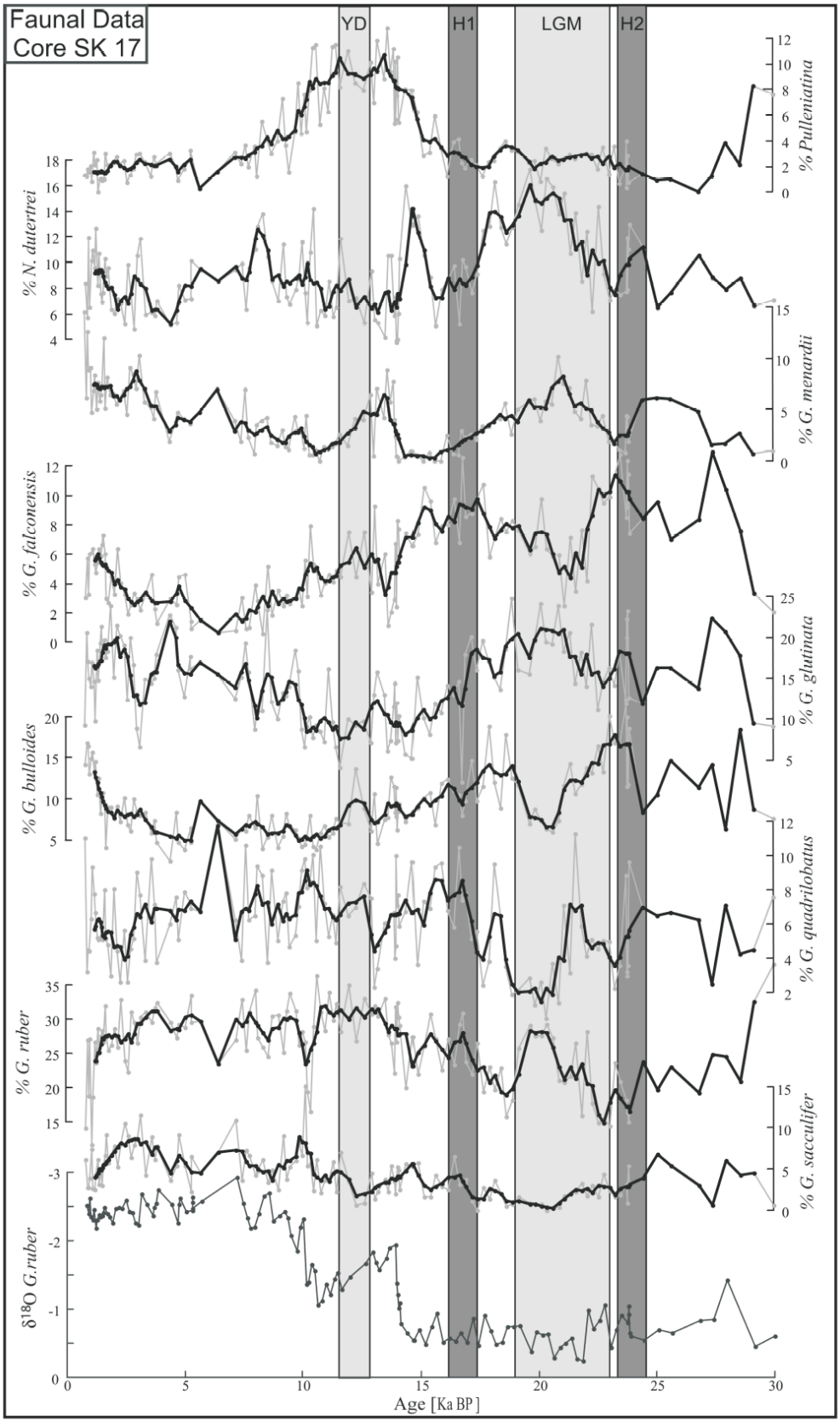

654

Figure 2 Singh et al

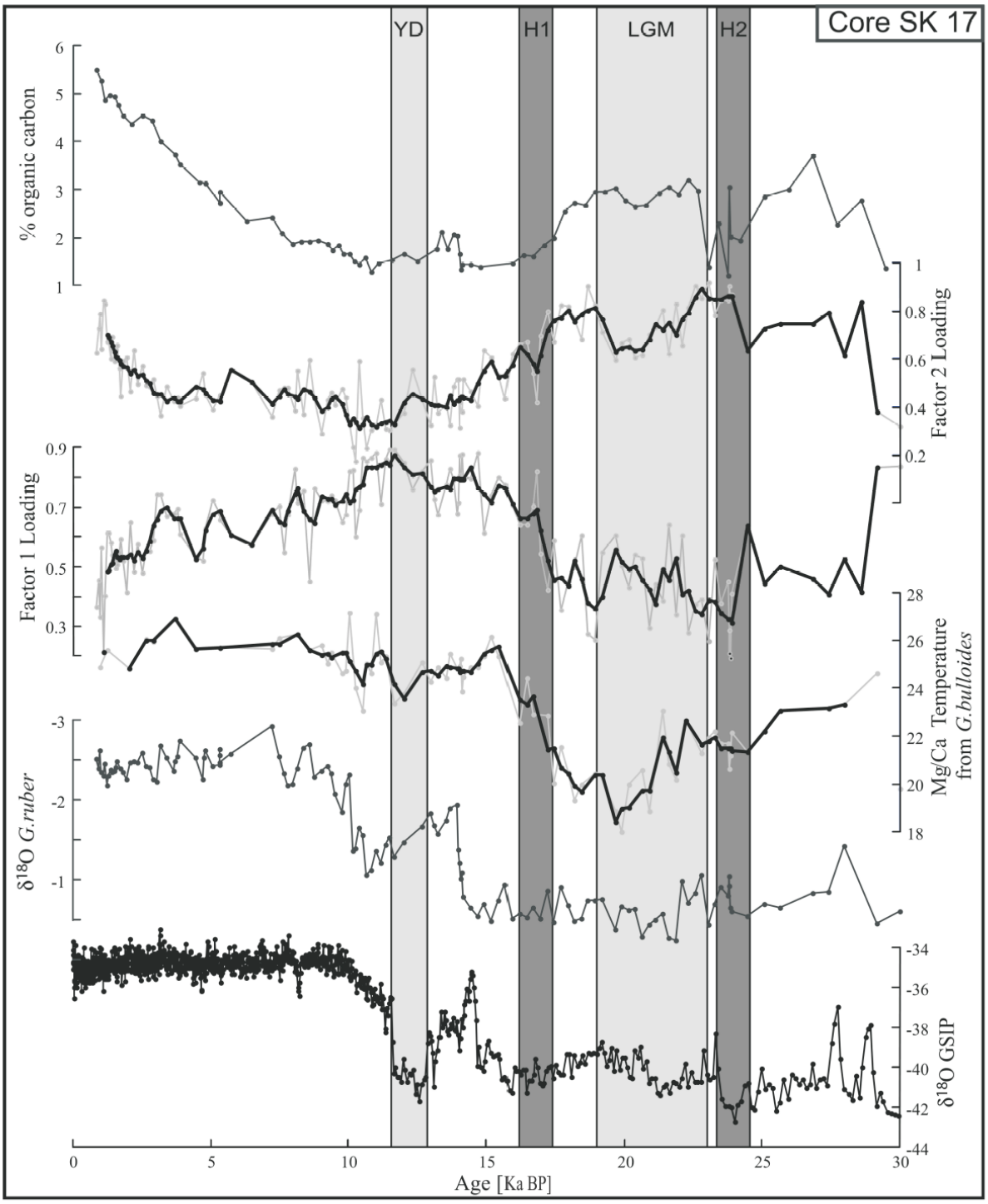

Figure 3 Singh et al

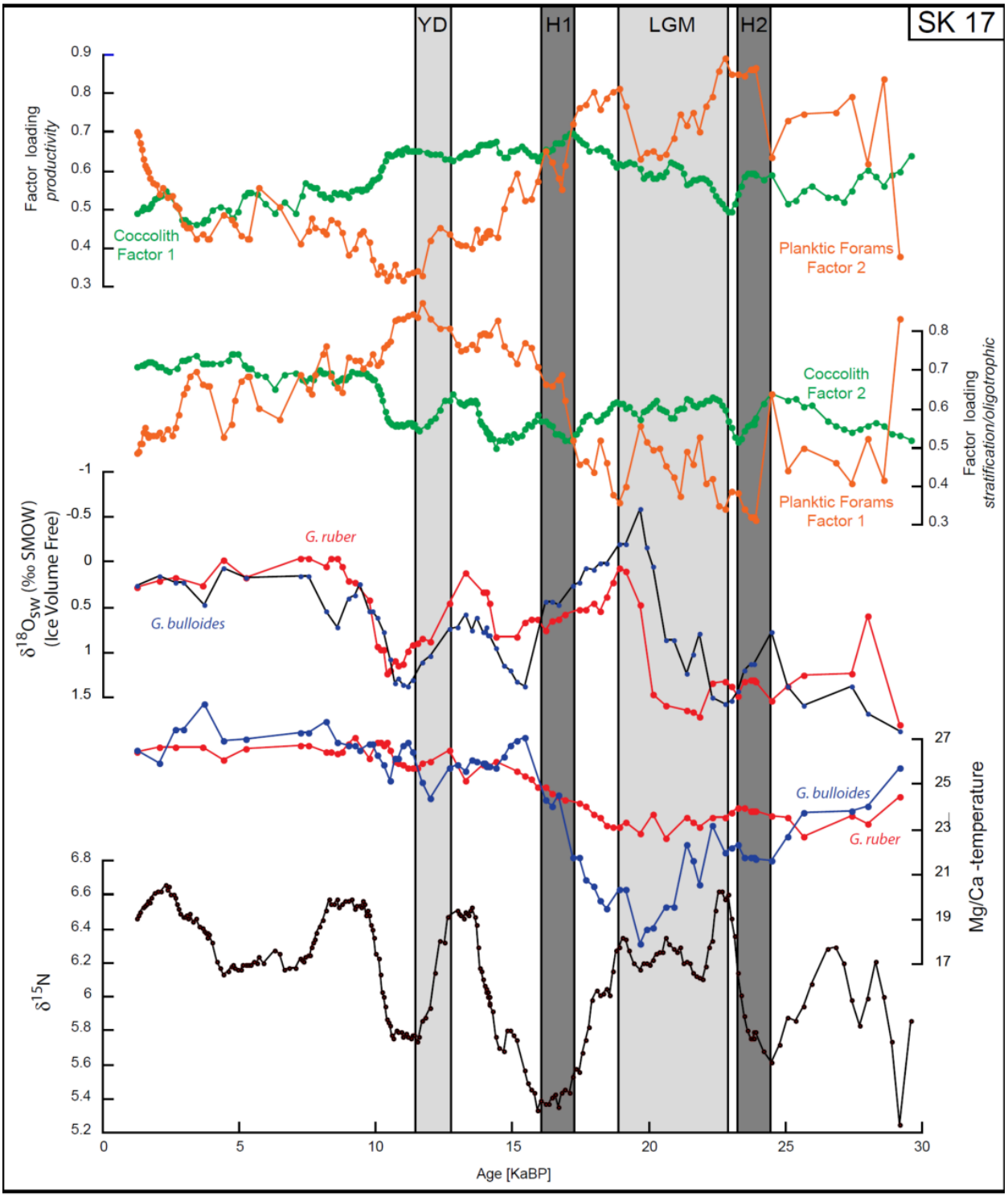

Figure 4 Singh et al

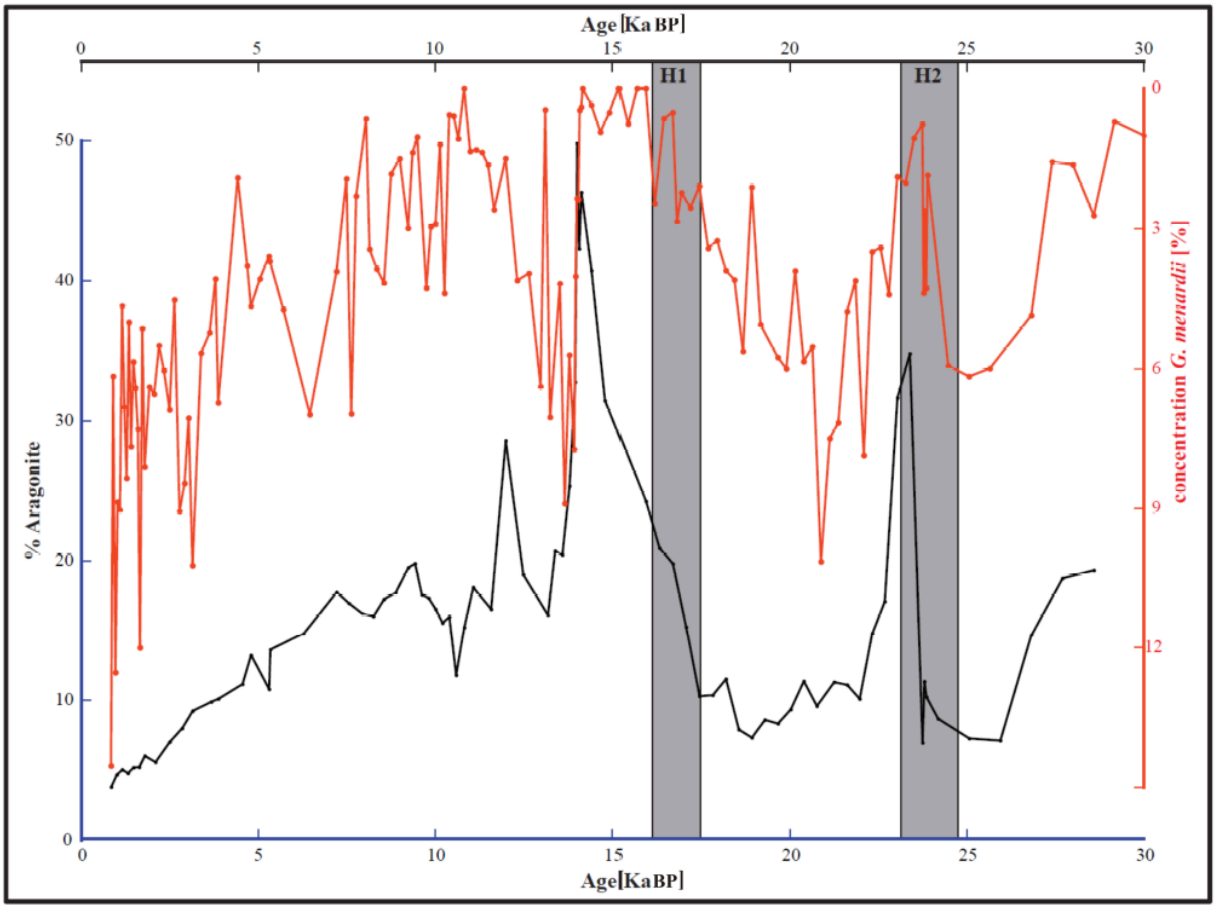

662 Figure 5 Singh et al